

**Fermilab**

TM-1385  
0300.000

SINGLE BUNCH INSTABILITIES OF THE RHIC BOOSTER

K.-Y. Ng

February 1986

SINGLE BUNCH INSTABILITIES OF THE RHIC BOOSTER

King-Yuen Ng

Fermi National Accelerator Laboratory

P. O. Box 500

Batavia, IL 60510

(February 1986)

I. INTRODUCTION

In this paper, we try to estimate the stability limits and impedances of the Brookhaven RHIC booster. Some important data of the booster are shown in Table I. From the stability limits listed in Table II and impedances in Table V, it is clear that the booster is safe against either fast microwave instabilities or slow mode-colliding single bunch instabilities.

II. STABILITY LIMITS

We group together the criterions for single-bunch stabilities. The bunch is assumed to be Gaussian in shape with RMS time spread  $\sigma_t$  and momentum spread  $\sigma_p$  per amu.

(a) Microwave instabilities with growth rate much faster than a synchrotron oscillation

If the driving longitudinal impedance  $Z_L$  or transverse impedance  $Z_T$  is a broad band with width much bigger than the frequency spread of the bunch  $\sigma_t^{-1}$  and centered at a frequency ( $\sim n$  times the revolution frequency) much bigger than  $\sigma_t^{-1}$ , the stability limits are<sup>1</sup>

$$\left| \frac{Z_L}{n} \right| < \frac{2\pi |\eta| (E/e)}{I_p} \left( \frac{\sigma_p}{p} \right)^2 \frac{A}{\mathcal{V}}, \quad (2.1)$$

$$\left| Z_T \right| < \frac{4\sqrt{2\pi} |\eta| (E/e)}{I_p \beta} \left( \frac{\sigma_p}{p} \right) \frac{A}{\mathcal{V}}, \quad (2.2)$$

where  $\bar{\beta}$  is the average beta function,  $p$  and  $E$  the particle momentum and energy per amu,  $A$  the atomic number,  $q$  the charge in units of  $e$ ,  $\eta = \gamma_t^{-2} - \gamma^{-2}$  the frequency dispersion parameter,  $\gamma_t$  the transition gamma,  $\gamma$  the particle energy in units of its rest mass, and  $I_p = qeN/\sqrt{2\pi}\sigma_z$  the peak current of the Gaussian bunch of  $N$  particles.

If the driving impedances are resonances at a frequency much bigger than  $\sigma_z^{-1}$  but with a width much less than  $\sigma_z^{-1}$ ,  $Z_L$  and  $Z_T$  in above represent only the effective impedances averaged over the bunch spectrum. Sometimes it is more convenient to rewrite Eqs. (2.1) and (2.2) as<sup>2</sup>

$$\frac{Z_L}{Q} < \frac{4|\eta|(E/e)}{I_{AV}} \left(\frac{\sigma_p}{p}\right)^2 \frac{A}{\beta}, \quad (2.3)$$

$$\frac{Z_T}{Q} < 8\sqrt{\frac{2}{\pi}} \frac{|\eta|(E/e)}{I_{AV}\bar{\beta}} \left(\frac{\sigma_p}{p}\right) \frac{A}{\beta}, \quad (2.4)$$

where  $Z_L$  and  $Z_T$  are the peak values,  $Q$  the quality factor of the resonance, and  $I_{AV}$  the average current of the bunch.

(b) Mode-coupling single bunch instabilities with growth rate much slower than a synchrotron oscillation

Oscillation modes of a single bunch will be shifted by coherent forces. When two of these modes collide, instability slow compared with a synchrotron oscillation can occur. These instabilities are driven by  $Z_L/n$  and  $Z_T$  averaged over the bunch spectrum at low frequencies. The limits for stability are<sup>3</sup>

$$\left|\frac{\bar{Z}_L}{n}\right| < \frac{8\sqrt{\pi}|\eta|(E/e)(\sigma_z/R)(\sigma_p/p)^2}{I_{AV}} \frac{A}{\beta} \quad (2.5)$$

$$\left|\bar{Z}_T\right| < \frac{4\sqrt{\pi}|\eta|(E/e)}{I_{AV}\bar{\beta}} \left(\frac{\sigma_p}{p}\right) \frac{A}{\beta}. \quad (2.6)$$

We take the 95% bunch length as 6 meters; so the RMS bunch length is  $\sigma_z = 600/2\sqrt{6} = 122.5$  cm. The RMS momentum spread is  $\sigma_p/p = \frac{25}{\sqrt{6}} \times 10^{-4}$  for proton

and  $\frac{1}{\sqrt{6}} \times 10^{-4}$  for all other ions at injection. The various stability limits of Eqs. (2.1)-(2.6) are computed at injection and are listed in Table II.

### III. ESTIMATE OF $Z_L$ AND $Z_T$ FOR THE BOOSTER

The RHIC booster consists of 36 dipoles each of length 2.7 m with semi-oval beam pipe 6.731 cm in height and 15.24 cm in width as shown in Figure 1. Between the dipoles are 36 units of circular beam pipe of radius 7.62 cm. Each of these circular beam pipe houses a beam monitor set, bellow ripples and goes through a quadrupole. Also there are nine circular pipes of radius 7.62 cm and length 4.5 m in the straight sections.

#### III.1 WALL RESISTIVITY

The semi-oval beam pipes inside the dipoles are approximated by a rectangular cross section 6.731 cm x 15.24 cm. The wall impedances of these beam pipes and the circular pipes can then be evaluated using standard formulas<sup>4</sup>. The contributions are

$$Z_L/n = (1 + j)1.2(\beta/n)^{\frac{1}{2}} \text{ ohms}, \quad (3.1)$$

$$Z_T = \begin{cases} (1 + j)0.043(\beta n)^{-\frac{1}{2}} \text{ M}\Omega/\text{m}, & \text{(vertical)} \\ (1 + j)0.024(\beta n)^{-\frac{1}{2}} \text{ M}\Omega/\text{m}, & \text{(horizontal)} \end{cases} \quad (3.2)$$

where  $\beta$  is the velocity of the bunch in units of  $c$  the light velocity and a conductivity of stainless steel  $\sigma = 0.14 \times 10^7$  mho/m is assumed. These impedances will be too small in the microwave region to drive any fast instability. Slow growths are driven by the average impedances seen by the bunch. These are obtained through multiplying the above by the factor  $\Gamma(\frac{1}{2})(\sigma_e/\pi R)^{\frac{1}{2}}$  leading to  $\text{Im } \bar{Z}_L/n = 0.46\beta^{\frac{1}{2}} \Omega$  and  $\text{Im } \bar{Z}_T = 0.017\beta^{\frac{1}{2}} \text{ M}\Omega/\text{m}$  for vertical and  $0.010\beta^{\frac{1}{2}} \text{ M}\Omega/\text{m}$  for horizontal. They are well below the theoretical limits in Table II.

### III.2 JOINTS BETWEEN DIPOLES AND BELLOW CONTRIBUTION

The joint between dipoles has two steps of  $7.62 - 3.37 = 4.25$  cm, which will contribute to the impedances. There will be also 15 to 20 bellow ripples on this 7.62 cm radius circular joint to allow for thermal expansion when the booster is run at  $\sim 200^\circ\text{C}$ . However, because the depth of the ripples 0.5 cm is small compared with the joint radius 7.62 cm, the electromagnetic fields can hardly go inside the ripples. As a result, these ripples will make nearly no contribution to the impedances. This conjecture has been checked by running the code<sup>5</sup> TBCI on a pill-box cavity with 15 ripples as shown in Figure 2(a) and also on the same cavity with the ripples removed as shown in Figure 2(b). The real parts of the longitudinal impedances are shown in Figures 3 and 4 respectively. We find no essential difference between the two figures. What we see are just sharp resonances of the cavity below cutoff. This indicates that the ripples give little or no contribution to the impedances.

Based on the above analysis, we can consider the circular joint as a simple pill-box cavity by ignoring all the bellow ripples. The length of this section is 1.5 m; so we expect the contribution to impedances will not be big as a result of transit-time effect. The code<sup>6</sup> URMEL is used to analyse all the resonances below cutoff. The semi-oval pipes attached to each side are approximated by circular pipes of radius  $b = 3.40$  cm having the same cutoff frequency. The results are shown in Tables III and IV for the monopole (longitudinal) and dipole (transverse) mode respectively. The transverse shunt impedance in the fourth column of Table IV is obtained from the longitudinal shunt impedance (second column) computed at a distance  $b = 3.40$  cm from the center axis of the pill-box by

$$\frac{Z_T}{Q} = \frac{c}{\omega_R b^2} \frac{Z_L}{Q}, \quad (3.3)$$

where  $f_R = \omega_R/2\pi$  is the resonance frequency. We see that the resonances are very closely spaced ( $\Delta \sim 0.0012$  to  $0.0080$  GHz) because of the long length of the joint. What the bunch sees will therefore be an average

$$(Z_L)_{\text{eff}} = \frac{\pi}{2} \cdot \frac{Z_L}{Q} \cdot \frac{f_R}{\Delta} m \quad (3.4)$$

for the longitudinal impedance and a similar formula for the transverse impedance. In above,  $m = 36$  is the total number of joints in the booster and  $\Delta$  the spacing of the resonances at  $f_R$ . These effective impedances are also listed in Tables III and IV. We see that the largest  $(Z_T)_{\text{eff}}$  is  $0.02 \text{ M}\Omega/\text{m}$ ; therefore fast head-tail growth is not possible. The largest longitudinal impedance is  $(Z_L)_{\text{eff}} \sim 4500$  around 2 GHz. The largest revolution frequency is  $f_0 = c/2\pi R = 0.00149$  GHz or the smallest harmonic corresponding to 2 GHz is  $n = 1345$ . Thus, the largest possible contribution to the longitudinal impedance per harmonic is  $(Z_L/n)_{\text{eff}} = 3.3 \Omega$ , which is well below the limit for fast microwave instability.

At low frequencies, we can estimate the impedances according to the following formulas<sup>7,8</sup>: ( $Z_0 = 377 \Omega$ )

$$\text{Im } Z_L/n = Z_0 \frac{0.241}{\beta R} \cdot \frac{b(d/b-1)^2}{d/b + 0.412}, \quad (3.5)$$

$$\text{Im } Z_T = \frac{Z_0}{\pi d} \cdot \frac{(d/b-1)^2}{0.45 + 0.39d/b}, \quad (3.6)$$

where  $b = 3.4$  cm and  $d = 7.62$  cm are the smaller and larger radii of the steps. For 36 circular joints we get  $\text{Im } \bar{Z}_L/n = 2.0/\beta \Omega$  and  $\text{Im } \bar{Z}_T = 0.066 \text{ M}\Omega/\text{m}$ , which are obviously below the limits for slow growths.

### III.3 BEAM POSITION MONITORS

There are  $M = 45$  sets of beam position monitors in the booster. Each set

consists of two triangular plates monitoring the horizontal position of the bunch and two triangular plates monitoring the vertical position. We approximate these four triangular plates by four cylindrical strips each of length  $\ell = 30$  cm and open angle  $2\varphi_0 = \frac{1}{2}\pi$ . At low frequencies or more precisely when  $n \ll R/\ell$ , we get<sup>9</sup>, for all the  $M=45$  sets,

$$\begin{aligned} Z_L/n &= 4MZ_c \left(\frac{\varphi_0}{\pi}\right)^2 \frac{\ell}{R} \left(\frac{n\ell}{R} + j\beta\right) \\ &= (j5.3\beta + 0.049n) \Omega, \end{aligned} \quad (3.7)$$

where  $Z_c$  is the characteristic impedance of the monitor which is assumed to be 50 ohms and matched to the termination impedance. The transverse impedance at low frequencies is approximately

$$Z_T \approx \frac{2R}{d^2} \frac{Z_L}{n} = (j0.058\beta + 0.005n) \text{ M}\Omega/\text{m}, \quad (3.8)$$

where  $d = 7.62$  cm is the radius of the circular beam pipe housing the monitors. We see that these impedances are too small to initiate slow growth instabilities.

If the plates are terminated at the ends, there will be no resonances at high frequencies. However, if the plates are terminated at the center, resonances can occur at frequencies  $f_R = mc/2\ell$ ,  $m = 1, 2, \dots$ , for both the longitudinal and transverse modes. Thus, the lowest resonance is at  $f_R = 0.5$  GHz. The shunt impedances and quality factors are<sup>9</sup>

$$Z_{sh} = Z_c^2 \frac{2\pi d\sigma\delta}{\ell}, \quad (3.9)$$

$$Q = \tau/\delta, \quad (3.10)$$

where

$$\tau = \frac{2\pi d Z_c}{Z_o} \quad (3.11)$$

is the electrical equivalent distance between the monitor and ground,  $\delta$  the skin depth,  $\sigma = 0.14 \times 10^7$  mho/m the conductivity of the monitor plates and  $Z_o = 377$  ohms. We get  $\tau = 6.35$  cm. Therefore, for  $M=45$  sets of monitors,  $Z_{sh}/Q = 716/m$  ohm and  $Q = 3340m^{\frac{1}{2}}$ . The transverse shunt impedance, if estimated using a formula like Eq. (3.8), gives  $Z_T/Q = 0.0059/m$  M $\Omega/m$ . When compared with the corresponding limits in Table III, it is evident that these resonances will not be big enough to drive any microwave instability.

#### III.4 KICKERS

The booster contains injection kicker, extraction kicker, and abort kicker. These kickers are of the form of window magnets of size 6 in x 2.6 in and total length  $\ell = 5.4$  m. The longitudinal and transverse impedances of such kickers have been estimated by Nassibian and Sacherer<sup>10</sup>. At low frequencies, they are

$$\frac{Z_L}{n} = \frac{Z_o x_o^2 \ell}{AR}, \quad (3.12)$$

$$Z_T = \frac{Z_o \ell}{A}, \quad (3.13)$$

where  $A$  is the area of the magnet cross section and  $x_o$  the displacement of the beam from the center of the magnet. Assuming a horizontal dispersion of 2 m and momentum spread 0.25%,  $x_o = 0.5$  cm. Then, for all the kickers,  $Z_L/n = 0.16 \Omega$  and  $Z_T = 0.002$  M $\Omega/m$ , which are of course negligibly small.

However, we would like to point out that, the above estimates are the impedances due to the induction of the magnet coils only. Usually, the vacuum chamber inside the kickers is of ceramic. Therefore, the image current of the beam is carried either by a thin metallic coating on the ceramic pipes or just the laminations of the magnets. Thus, a high wall impedance is possible. This can usually be avoided by having metallic rods at the outside of the ceramic pipes

### III.5 SUMMING UP

The impedances due to wall resistivity, dipole joints, beam monitors, and kickers are listed in Table V. They are small compared with the limits in Table II and will not cause instability of any sort.

There are other discontinuities in the booster that can contribute to the impedances but have not been included here. For example, the septum and the RF. The RF may contribute sharp resonances and lead to coupled bunch instabilities. However, this can usually be avoided by damping the important driving parasitic modes or by a feed-back system.

## REFERENCES

1. R. D. Ruth and J. M. Wang, IEEE Trans. Nucl. Sci. NS-28, 2405 (1981);  
S. Krinsky and J. M. Wang, BNL Report BNL-33867.
2. If we include only the real part of the resonance impedance and let  $Q$  tend to infinity, Eq. (2.3) follows from Eq. (2.1) immediately. However, the neglect of the imaginary part which carries a long tail is a violation of causality. Similar comment is applied to Eq. (2.4).
3. R. D. Ruth, Proc. of the Workshop on Accelerator Physics Issues for a Superconducting super Collider, Ann Arbor, MI, 1983, p. 151.
4. K. Y. Ng, Particle Accelerators 16, 63 (1984).
5. T. Weiland, DESY 82-015, 1982.
6. T. Weiland, DESY M-82-24, 1982.
7. E. Keil and B. Zotter, Particle Accelerators 3, 11 (1972).
8. K. Y. Ng, Fermilab Report FN-389.
9. A. G. Ruggiero, P. Strolin, and V. G. Vaccaro, CERN Report ISR-RF-TH/69-7.
10. G. Nassibian and F. Sacherer, CERN/ISR-TH/77-61.

Table I. Booster Parameter List

---

Injection energy, Au <sup>+33</sup>	1 MeV/amu
Top energy, Au <sup>+33</sup>	321 MeV/amu
B <sub>p</sub>	16.668 T·m
Circumference	201.75 m
Periodicity	6
Number of FODO cells	24
Cell length	8.41 m
Phase advance/cell	71°
Tune, horizontal & vertical	4.75
Beta, maximum/minimum	14.5/3.7 m
Dispersion, maximum	2.3 m
Transition energy, Y <sub>T</sub>	4.5
Betatron acceptance	50π mm·rad
Dipole field	1.2 T
Dipole length	2.4 m
Dipole gap	8.26 cm
Number of dipoles	36
Number of quadrupoles	48
Quadrupole length	0.5 m
Quadrupole bore radius	8.26 cm
Peak rf voltage, h = 1	15 kV
rf frequency, h = 1	71-200 kHz
rf frequency, h = 3	200-995 kHz
Repetition rate	1 sec <sup>-1</sup>
Vacuum, N <sub>2</sub> equivalent	10 <sup>-10</sup> Torr

---

Table II. Single-bunch stability limits of the RHIC booster

	p	d	C	S	Cu	I	Au
Atomic number A	1	2	12	32	63	127	197
Average charge q	1	1	6	14	29	29	29
$N_{sc}$ ( $10^9$ ), 3 bunches	5000	100	22	6.7	4.7	3.2	2.2
$\beta_{inj}$	0.566	0.177	0.126	0.100	0.078	0.060	0.046
$E_{inj}/amu$ (GeV)	1.138	0.953	0.946	0.943	0.941	0.940	0.939
$\sqrt{6(\sigma_p/p)_{inj}}$ ( $10^{-4}$ )	25	1	1	1	1	1	1
$\sigma_\tau = \sigma_z/\beta c$ (ns)	7.21	23.1	32.4	40.8	52.3	68.0	88.7
Fast grow limits							
broad band $ Z_L/n $	318 $\Omega$	199 $\Omega$	213 $\Omega$	434 $\Omega$	363 $\Omega$	1400 $\Omega$	3210 $\Omega$
$ Z_T $	71 M $\Omega/m$	3360 M $\Omega/m$	5310 M $\Omega/m$	13700 M $\Omega/m$	14700 M $\Omega/m$	73500 M $\Omega/m$	22000 M $\Omega/m$
narrow res. $Z_L/Q$	13300 $\Omega$	8333 $\Omega$	8920 $\Omega$	18200 $\Omega$	15200 $\Omega$	58500 $\Omega$	134000 $\Omega$
$Z_T/Q$	2.1 M $\Omega/m$	32.6 M $\Omega/m$	34.8 M $\Omega/m$	71.0 M $\Omega/m$	59.6 M $\Omega/m$	229 M $\Omega/m$	525 M $\Omega/m$
Slow grow limits							
$ \bar{Z}_L/n $	1800 $\Omega$	1130 $\Omega$	1210 $\Omega$	2450 $\Omega$	2050 $\Omega$	7920 $\Omega$	18200 $\Omega$
$ \bar{Z}_T $	2.3 M $\Omega/m$	36.2 M $\Omega/m$	38.7 M $\Omega/m$	78.8 M $\Omega/m$	66.1 M $\Omega/m$	254 M $\Omega/m$	584 M $\Omega/m$

Note: (1)  $N_{sc}$  is the maximum number of particles in booster allowed by space charge.  
(2)  $\sigma_\tau$  is the RMS time spread and  $\sigma_p$  the RMS momentum spread per amu of a bunch.

Table III. Resonances of a bellow-joint (monopole modes)

$f_R$ (GHz)	$Z_{sh}/Q$ ( $\Omega$ )	Q	$Z_{eff} = 36 \cdot \frac{\pi}{2} \frac{Z_{sh} f}{Q \Delta}$ ( $\Omega$ )
1.508	0.049	6626	464
1.517	0.075	6624	559
1.531	0.562	6625	2780
1.552	0.0002	6632	0.88
1.579	1.120	6651	3390
1.611	1.050	6682	2733
1.649	0.013	6728	30.3
1.691	1.545	6787	3283
1.739	2.191	6859	4309
1.792	0.632	6943	1175
1.848	0.082	7036	148
1.908	1.423	7138	2476
1.972	2.590	7248	4443
2.038	2.251	7363	3815
2.108	1.017	7531	1707
2.180	0.111	7609	187
2.254	0.121	7737	206
2.330	0.840	7866	1437
2.408	1.727	7997	2977
2.488	2.339	8128	4414
2.569	2.494	8257	4473
2.650	2.243	8381	4115
2.733	1.748	8499	3255
2.816	1.184	8605	2258

Note: (1) Q is computed with conductivity  $\sigma = 0.14 \times 10^7$  mho/m.  
(2)  $f_{cutoff} = 3.38$  GHz (TM mode).  
(3)  $Z_{eff}$  is the average longitudinal impedance for 36 joints.

Table IV. Resonances of a bellow-joint (dipole modes)

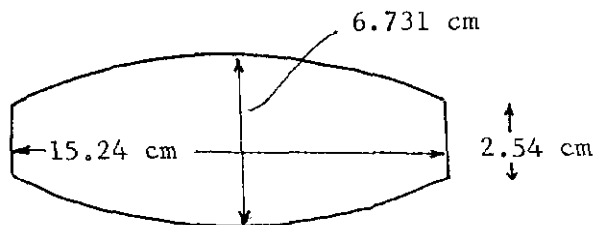
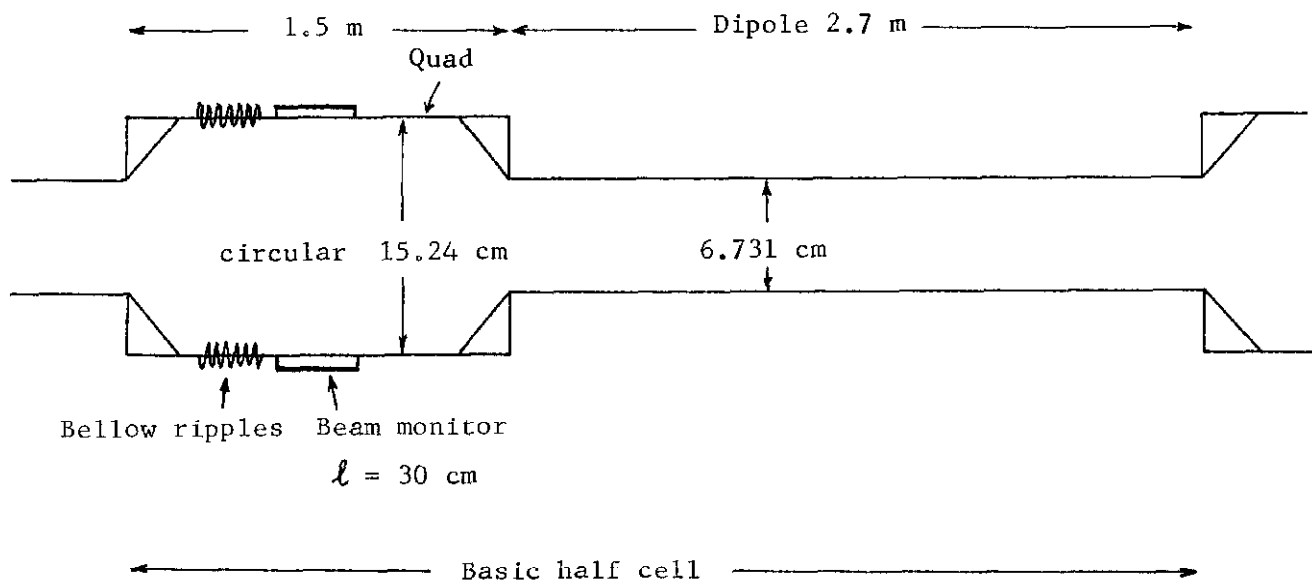
$f_R$ (GHz)	$Z_{sh}/Q$ ( $\Omega$ )	Q	$Z_T/Q$ ( $\Omega/m$ )	$(Z_T)_{eff} = 36 \times \frac{\pi}{2} \frac{Z_T f}{\Omega \Delta}$ ( $\Omega/m$ )
1.157	0.004	4324	0.14	654
1.171	0.002	4412	0.017	261
1.193	0.024	4557	0.831	2954
1.222	0.056	4756	1.89	3899
1.260	0.001	5006	0.033	57
1.304	0.078	5301	2.47	3875
1.354	0.210	5637	6.41	9260
1.410	0.143	6006	4.19	5760
1.470	0.007	6401	0.197	264
1.534	0.085	6813	2.29	3010
1.602	<b>0.385</b>	<b>7235</b>	<b>9.93</b>	12940
1.673	0.660	7654	16.29	21400
1.746	0.683	8056	16.2	21620
1.821	0.438	8427	9.93	13544
1.879	0.118	8747	2.57	<b>3580</b>
1.975	0.008	8995	0.167	239
2.053	0.329	9151	6.62	9853
2.131	1.078	9201	20.89	32482
2.208	1.918	9146	35.88	58561
2.284	2.186	9081	39.53	65040

- Note: (1) Q is computed with conductivity  $\sigma = 0.14 \times 10^7$  mho/m  
(2)  $Z_{sh}$  is the longitudinal shunt impedance computed at 3.4 cm from the joint axis.  $Z_T$  is the transverse shunt impedance.  
(3)  $(Z_T)_{eff}$  is the average transverse impedance for 36 joints.  
(4)  $f_{cutoff} = 2.58$  GHz (TE mode)

Table V. Total impedances of the RHIC booster

	Low frequency average		Microwave region broad band ( $Z_L/n$ , $Z_T$ ) narrow resonance ( $Z_L/Q$ , $Z_T/Q$ )
	$Z_L/n$ ( $\Omega$ )	$Z_T$ (M $\Omega$ /m)	
Wall resistivity	0.46	.017 (.010)	
Bellows and joints	2.0	0.066	$Z_L/n = 3.3 \Omega$ $Z_T = 0.02 \text{ M}\Omega/\text{m}$
Beam monitors	5.3	0.058	$Z_L/Q = 716 \Omega$ $Z_T/Q = 0.0059 \text{ M}\Omega/\text{m}$
Kickers	0.16	0.002	
Total	7.9	.143 (.137)	

Note: Whenever the vertical and horizontal transverse impedances are different, the horizontal one is enclosed in brackets.



Beam pipe cross section inside dipole

Figure 1

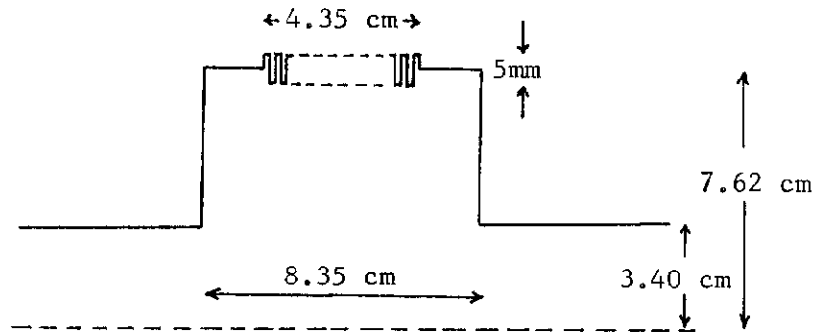


Figure 2(a) There are in total 15 bellow ripples of period 3 mm and depth 5 mm.

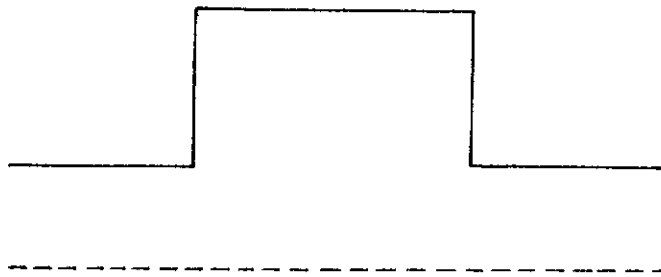


Figure 2(b) Same as (a) but with all bellow ripples removed.

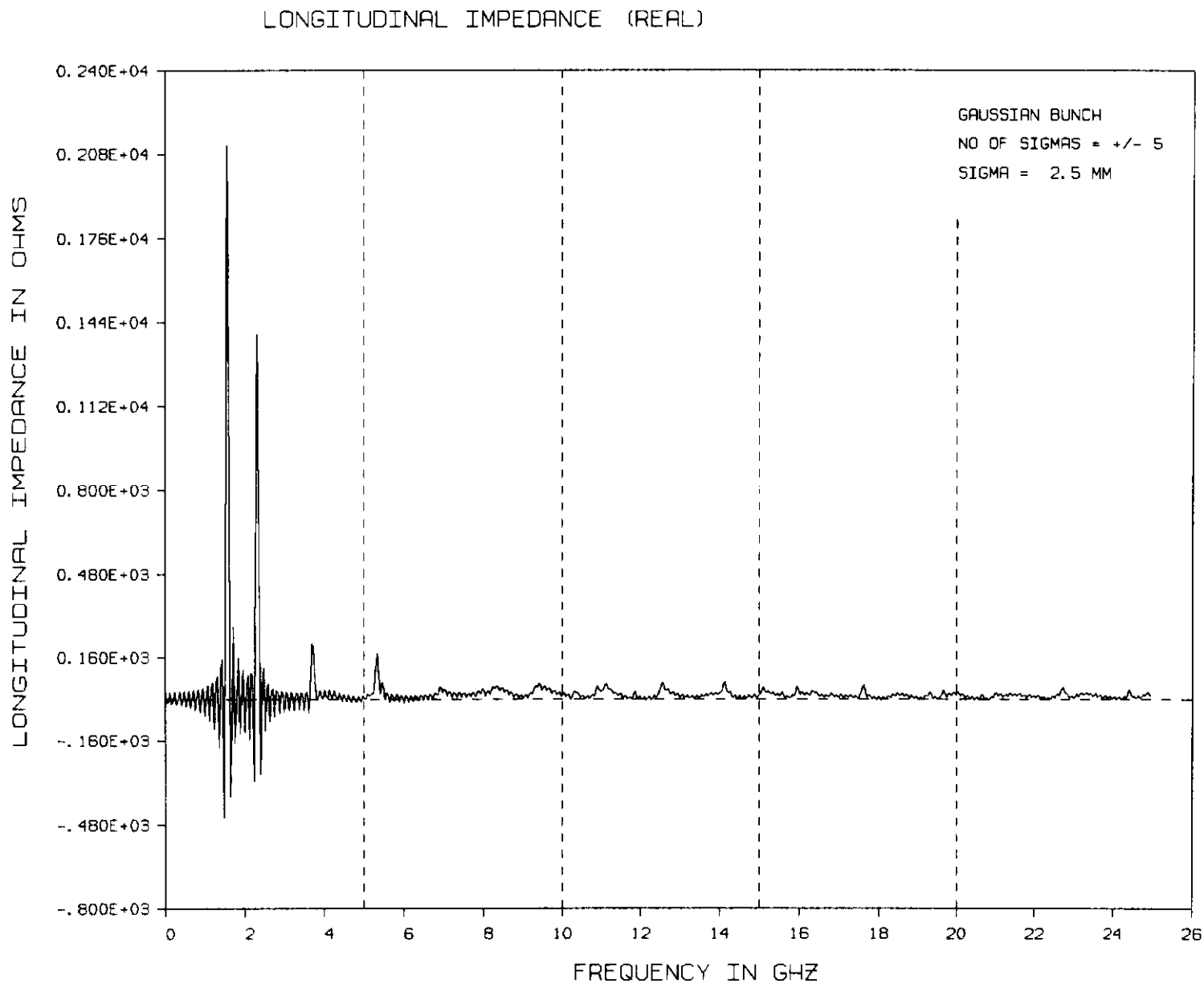


Figure 3. Longitudinal impedance of the cavity with ripples as in Figure 2(a). The ripples in this plot is due to the truncation of the wake potential which is almost periodic.

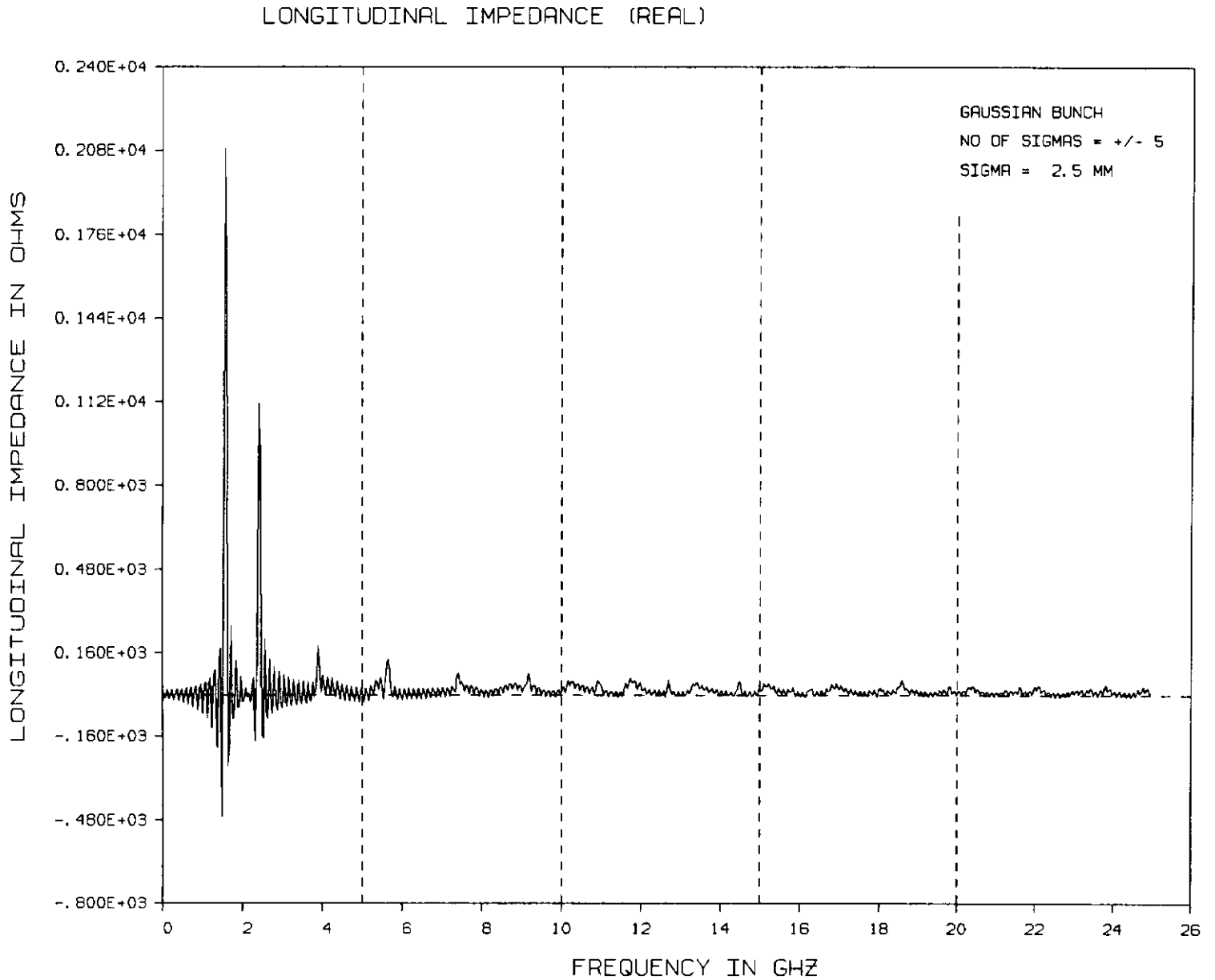


Figure 4. Longitudinal impedance of the cavity without ripples as in Figure 2(b). The ripples in this plot is due to the truncation of the wake potential which is almost periodic.